ORIGINAL PAPER

Evaluating the effect of ocean-atmospheric indices on drought in Iran

Maryam Mohammadrezaei[1] · Saeed Soltani[1,2] · Reza Modarres[1,2]

Abstract
This study investigated the relationship between ocean-atmospheric indices and drought in Iran. Using > 30-year precipitation data from 37 synoptic stations (ending 2015), standard precipitation index (SPI) was calculated for periods of 1-, 3-, 6-, 9-, 12-, 15-, 18-, 24-, and 48-month time scales. A set of monthly ocean-atmospheric oscillations (OA) indices including Antarctic Oscillation (AAO), Arctic Oscillation (AO), Atlantic Multi-Decadal Oscillation (AMO), North Atlantic Oscillation (NAO), El Nino Southern Oscillation (ENSO): (NINO 1.2, NINO 3, NINO 3.4, NINO 4, SOI), and Western Mediterranean Oscillation (WeMo) were also included in our analysis. The simultaneous relationship between SPI and ocean-atmospheric oscillations was investigated using Spearman's correlation test. The cross correlation function (CCF) coefficient was also utilized to investigate their asynchronous relationships at 1-, 3-, 6-, 9-, 12-, 15-, 18-, 24-, 48-month lag time. Finally, the multivariate linear regression was used to model the end relationships among SPI time-scales and OA indices. AMO and NINO 4 had the most significant and most frequent relationship with SPI in the western and northern parts of Iran. Except for southeastern parts, AMO, NINO 3.4, and NINO 4 had the most significant and most frequent relationship with SPI. Moreover, results showed that asynchronous relationships outperformed simultaneous ones. AMO was recognized as the most important index in modeling the relationship between drought and OA indices across all stations with high potentials to be used for predicting climatic conditions and drought management in Iran.

Keywords SPI · Ocean-atmospheric indices · Simultaneous and asynchronous relationship · Iran

1 Introduction

Drought is a natural hazard that can have severe and long-lasting impacts on natural and human systems. It occurs in response to rainfall reduction and usually lasts for one or more seasons. Hence, gaining insights into drought and its connection with other atmospheric anomalies have significant implications for water resource planning, management, and drought prediction sentence:(Lyon 2005, Shimizu & Ambrizzi 2015, Lim & Kim 2007). The link between climatic signals, ocean-atmospheric (OA) oscillations and other atmospheric events such as precipitation and drought offers great capabilities for analysis and prediction of drought and other climatic disasters.

These oscillations contribute significantly in controlling climate changes in many regions Ghasemi and Khalili (2008). Generally, ocean-atmospheric oscillations occur when the sea-level pressure and sea surface temperature (SST) differ between two oceanic locations (poles); in other words, increasing pressure or SST in a location leads to its decrease elsewhere. The pressure difference between the two poles has a useful application for the quantitative explanation of these oscillations (Partridge 2001). The availability of long-term statistics for these variables also highlights their usefulness for predicting and assessing drought trends in any region. The US National Oceanic and Atmospheric Administration has developed an array of indices to investigate atmospheric oscillations by estimating the difference in pressure and temperature over oceanic areas (Negaresh and Armesh 2011). These indices represent the most important phenomena that are caused by ocean-atmosphere and land-based interactions, which are the result of annual climate variability such as drought on the Earth's surface. Drought studies essentially require long-term climatic and hydrological data, while without these data, it would be impossible to study on the field. Rainfall is the foremost factor in controlling, creation, expansion, and durability of

✉ Saeed Soltani
  ssoltani@cc.iut.ac.ir

1 Department of Natural Resources, Isfahan University of Technology, Isfahan 8415683111, Iran

2 Center of excellence on risk management and natural hazards, Isfahan University of Technology, Isfahan 8415683111, Iran

droughts (Oladipio 1985). The standardized precipitation index (SPI) is a rainfall-based index whose validity and accuracy have been acknowledged by many researchers.

The relationship between ocean-atmospheric oscillation indices and drought is analyzed using two procedures: simultaneous and asynchronous correlation analyses. The former procedure evaluates the effect of oscillations on drought during a certain period while the latter investigates the time lag effect of ocean-atmospheric oscillations on drought over monthly timescales. Iran, like many countries in the Middle East and North Africa, due to geographical and climatic situations, does not have sufficient water supplies. Given the severe oscillation in rainfalls, the occurrence of droughts is inevitable in the country and indicates the possibility of more droughts in the future than in the past (Darand 2014, Nikzad & Behbahani khub 2013). Inefficient management with inappropriate strategies will waste existing resources and intensify devastating effects of drought. A large body of studies has investigated the effect of atmospheric oceanic oscillations on precipitation and drought across the world, including Iran. For instance, Komuscu (2001) investigated the relationship between recent drought events and atmospheric circulation patterns in Turkey and found NAO exerted significant impacts on recent precipitation and drought events. Nazemosadat and Ghasemi (2002) assessed drought and its association with ENSO in Sistan-Baluchistan Province, southeastern Iran. They showed that La Nina and El Nino led to decreasing and increasing autumn precipitation, respectively, with varying magnitudes at different stations. Roughani et al. (2010) assessed the relationship between monthly and seasonal rainfall in Iran using SOI (southern oscillation index) and SST indices of the Pacific and Indian oceans. Their results showed that the SOI index in summer had a significant and robust relationship with the precipitation of October and autumn in the western and northwestern parts of Iran as well as the west coast of the Caspian Sea, so that the El Nino (negative) and La Nina (positive) phases often decrease and increase precipitation in these areas, respectively. In a study on the relationship between NAO and winter precipitation in Hungary, Matyasovszky (2003) showed that NAO occurred in the warm and cold phases during drought and wet periods, respectively.

Moreover, the results showed that NAO had a strong inverse correlation with winter precipitation and winter temperature. Jafarzadeh et al. 2009) investigated the effect of El Nino Southern Oscillation (ENSO) across the northwestern parts of Iran (Ardabil Province) during dry and wet periods and found a weak correlation between precipitation and ENSO. They also found that precipitation was more influenced by the topo-climatic conditions of the region and its surrounding areas.

Furthermore, El Nino (ENSO's warm phase) reduces summer rainfall while La Nina (ENSO's cold phase) reduces precipitation at all seasons. Dezfuli et al. (2010) showed that SOI and NAO had a negative correlation with autumn precipitation (July–August) in southwestern Iran. Azhdari Moghaddam et al.

(2012) studied drought using a neuro-fuzzy model and climatic indices, including precipitation and drought in southeastern Iran (Zahedan City). Their results showed, in simultaneous correlation relationship analysis, that rainfall and Nino 3 with $R^2 = 0.97$, 0.75, and error = 0.13, 0.33 were the most important input variables, while in one-month lag time correlation analysis, rainfall, SPI, and AMO were the most important variables, respectively. Mokhtari et al. (2012) assessed the relationship of NAO and SOI with RDI (Reclamation Drought Index) and SPI using correlation relationship analysis showed that the highest correlation coefficients were in northern parts of Iran, due to adjacency to the Caspian Sea as well as being affected by precipitation and drought from oceanic oscillations. In another study, Salahi and Hajizadeh (2013) concluded that the North Atlantic Oscillation (NAO) was more correlated with precipitation and temperature in western Iran (Lorestan province) in cold months of the year. Moreover, the positive phase of this index was related to droughts that occurred in the Aligudarz region and the wet period occurred in the Borujerd region. Khosravi (2004) studies the importance of the occurrence of intermittent drought in southeastern Iran (Sistan and Baluchestan provinces) and its relation to macro-scale atmospheric rotation patterns of the Northern Hemisphere. Using 20 teleconnection indices, he concluded that about 70% of the variability in drought could be explained by teleconnection patterns. In addition, the variability of indices such as ENSO and SST during the nineteenth and twentieth centuries was considered as the most effective factors contributing to drought in the USA (McCabe et al. 2008).

Previous studies have focused more on the relationship between precipitation and ocean-atmospheric oscillations and also on the relationship of these oscillations with the drought using one or more finite ocean-atmospheric indices. While drought is one of the phenomena affecting different aspects of human life, studies showed that teleconnection patterns in some parts of the world are connected with small-scale climate variation in other regions. Therefore, teleconnection patterns can be used to explain climate behavior Yarahmadi and Azizi 2008. These descriptions highlight the need to evaluate the teleconnection impacts of ocean-atmospheric oscillations on drought in Iran, as one of the most drought-affected regions in the world. Hence, an attempt is made in this study to comprehend the simultaneous and asynchronous relationship between effective ocean-atmospheric indices and drought occurrence for investigating the possibility of developing drought prediction models.

2 Materials and methods

2.1 Study area

Iran, with an area of 1,648,198 Km², is located in the southwest of Asia between 25.3° and 39.47° N longitude and

44.45° and 63.18° E latitude. Except for northern coastal and western mountainous areas, an arid and semi-arid climate dominates Iran (Raziei et al. 2005). Two large mountain chains including Alborz running from the northeast to the northwest and Zagros stretched from the northwest to the southeast, control the spatio-temporal distribution of precipitation in Iran. Precipitation decreases gradually from the north, northwest, and west towards the center, east, and south of the country (Halabian 2016).

Precipitation in Iran ranges annually from 50 (in deserts) to 1800 mm (in northern parts), with a mean of about 260 mm and coefficient of variation of 18 to 75% (Modarres 2006; Dinpashoh et al. 2004). An isohyetal of 250 mm separates low and high precipitation areas. The precipitation distribution varies significantly so that 61% of the country receives annual precipitation less than 250 mm while only 4% gets annual precipitation more than 600 mm. Precipitation also differs among seasons. Except for northern Iran, precipitation occurs mostly from October to June, especially from November to May (Masoudian 2011). Masoudian (2011) showed that precipitation centers are formed at the moisture uprising location from the Red Sea and Cyprus Sea to the lower and middle layers of the atmosphere and moved to southern and central Zagros regions and west parts of the Persian Gulf.

2.2 Data

2.2.1 Rainfall

Monthly rainfall data were obtained from 37 synoptic stations of the Iranian Meteorological Organization (www.irimo.ir 2016) with a statistical period of up to 30 years (from the establishment to 2015). Fig. 1 shows the name and geographical location of the synoptic stations.

2.2.2 Ocean-atmospheric indices

One method to study the teleconnection relationship between distant locations is the application of climate signals which provide useful means for predicting and estimating climate changes. Large-scale climatic signals are referred to as the atmospheric and/or ocean patterns which are initially formed in a particular geographical location and have the name of that location. Frequently, large-scale climate indices are generally categorized into teleconnection patterns, atmospheric patterns, precipitation, ENSO, Pacific Ocean surface temperature, and Atlantic Ocean surface temperature. In the present study, the NAO teleconnection index, AMO (Atlantic Multi-Decadal Oscillation) Index, ENSO Nino 1 + 2, Nino 3, Nino 3.4, and Nino 4, AAO, AO, WeMo, and SOI (NOAA, 2012) were obtained from www.cpc.ncep.noaa.gov 2017, www.esrl.noaa.gov/psd/data/climateindices/list 2017, and www.bom.gov.au/climate 2017 (Table 1).

2.3 Methods

At first, SPI was calculated for 1-, 3-, 6-, 9-, 12-, 15-, 18-, 24-, 48-month periods. Then, the simultaneous relationship between SPI and ocean-atmospheric indices at the stations was assessed using Spearman's correlation test. Moreover, cross-correlation function (CCF) was utilized to assess the lag time relationship (from 1 to 48 months) between SPI and atmosphere oceanic variables. For each lag time, we drew the boxplot of ocean-atmospheric indices at each station (333 boxplots for 37 stations and 9 lag times). Finally, the stepwise regression model was utilized to predict the simultaneous and lag time (1, 2, 3, 4, 5, 6, 12, 24, and 48 months) effect of ocean-atmospheric indices on SPI. The performance of the models was evaluated by root mean squared error (RMSE), coefficient of efficiency (CE), r-squared statistics (coefficient of determination, Pearson's r squared) (r^2), and r. The best significant models were selected by F test, the test of significance level, and error metrics (highest CE, R and R^2, and lowest RMSE) (https://www.co-public.lboro.ac.uk/cocwd/HydroTest/Details.h). The details of these indices are described in the following.

2.3.1 Standardized precipitation index (SPI)

This index is calculated based on the cumulative probability of precipitation over different time scales from one month to over a year. This time scale should be fitted to a proper statistical distribution. Thom (1958) found that the Gamma function was fitted to rainfall time series data in many parts of the world; therefore, McKee et al. (1993) developed SPI based on the gamma distribution. Since the gamma function is not defined for value 0 and the precipitation value may be 0, a modified gamma distribution function (cumulative) is required to include a value of zero. In the next step, this cumulative probability distribution is transformed into a standard normal distribution (Z or SPI) with zero mean and one standard deviation. SPI is calculated using the Abramowitz-Stegun approximation which transforms the cumulative probabilities to the standard normal random variable (Z).

2.3.2 Multivariate regression

The multivariate regression (Eq. 1) is utilized to predict the simultaneous and time lag effect of various ocean-atmospheric indices on SPI:

$$\text{SPI}_i = \alpha_1 \text{OA}_{jk} + \alpha_2 \text{OA}_{jk} + ...\alpha_n \text{OA}_{jk} + \beta \qquad (1)$$

where i is time scale (0-, 1-, 3-, 6-, 9-, 12-, 15-, 18-, 24-, and 48-month time lag), β is the intercept in the equation, α_1 to α_n are the equation coefficients, and OA_{jk} is the ocean-atmospheric index in which j represents the type of index and k denotes lag time in month. The R, R^2, CE, and RMSE statistics are then utilized to evaluate the predictive performance of the models.
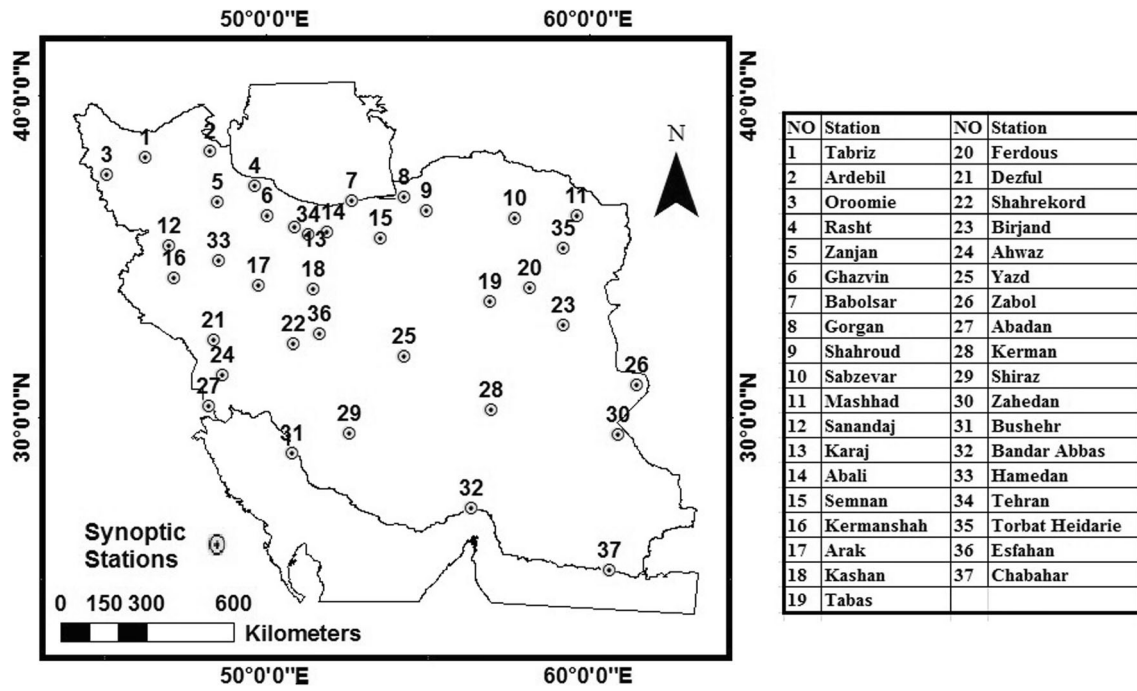
Fig. 1 Geographical locations of Synoptic Stations in Iran. Numbers are referred to stations in table

2.3.3 Cross-correlation function

Cross-correlation investigates the similarity between two variables as a function of lag time. In this method, the autocorrelation function shows the correlation of variables with the previously occurring variables. If the graph has a steep slope, then the events have a short-term relationship, while low slopes signify a long-term relationship between the variables. CCF can be formulated as follows (Salas 1993) (Eq. 2):

$$r_k = \frac{\sum_{t=1}^{N-K} \left(X_t - \overline{X}\right)\left(X_{t+k} - \overline{X}\right)}{\sum_{t=1}^{N} \left(X_t - \overline{X}\right)^2} \tag{2}$$

where r_k is the cross-correlation of lag k, which similar to correlation coefficient statistic, ranges from -1 to 1. N is the total number of data and $\overline{X}$ is average values.

3 Results

3.1 Simultaneous relationship

At most stations, the simultaneous relationship between ocean-atmospheric indices and SPI was not statistically significant. The highest correlation coefficient was found for Bushehr station between 3-month NINO 1.2 and SPI in January. Moreover, SPI was not significantly correlated with

Table 1 Indicators of climate in current study

Climate indicator		
AAO	Antarctic Oscillation	
AMO	Atlantic Multi-Decadal Oscillation	
AO	Arctic Oscillation	
NAO	North Atlantic Oscillation	
NINO 1 + 2	ENSO	Extreme Eastern Tropical Pacific SST
NINO 3		Eastern Tropical Pacific SST
NINO 3.4		East Central Tropical Pacific SST
NINO 4		Central Tropical Pacific SST
SOI	Southern Oscillation Index	
WeMo	Western Mediterranean Oscillation	

the ocean-atmospheric indices at 7 stations located in the north (Rasht, Semnan, Urmia, Gorgan, Mashhad, Torbat Heydariyeh, and Sabzevar), 5 stations in the south (Bandar Abbas, Chabahaar, Zabol, Zahedan, and Kerman), 5 stations in the center (Arak, Yazd, Isfahan, Kashan, and Tehran), and 2 stations in the west (Shiraz and Hamedan). For other stations, SPI was significantly correlated with AAO index in January, February, and December; with AMO and NINO 1.2 indices over all months; with AO in April, August, and November; with NAO in January, April, August, and December; with NINO 3 in all months except December; with NINO 3.4 in all months except May, October, November, and December; with NINO 4 in all months except October–December, with SOI in all months except May, June, November, and December; and with WeMo in April, June, September, and October.

AAO, AO, and SOI were negatively, and NAO and WeMo were positively correlated with SPI. The relationship between SPI and other indices was either negative or positive. Fig. 2a—j represent the geographic distribution of the stations with significant simultaneous relationships found between SPI and AAO, AMO, AO, NAO, NINO 1.2, NINO 3, NINO 3.4, NINO 4, SOI, and WeMo indices in Iran, respectively. Accordingly, the simultaneous relationship of SPI was significant only with AMO and NINO 4 in the north and west of Iran, respectively.

3.2 Asynchronous relationships

In this method, the asynchronous relationship refers to the monthly difference between ocean-atmospheric anomalies and drought occurrence. The correlation coefficients of asynchronous relationships were lower than those of simultaneous relationships. The number of stations with a significant relationship was higher in lag time analysis than that in simultaneous analysis.

In addition, the correlation coefficients decreased at most stations by increasing lag time and only AMO, NINO 1.2, NINO 3, NINO 3.4, and NINO 4 indices were correlated significantly with SPI at all stations. These correlation coefficients were positive in short-term lags and negative in long-term lags. The relationship of AAO, AO, NAO, SOI, and WeMo indices was not significant with SPI in any of the lag times and stations. Furthermore, NINO 3.4 and NINO 4 were positively correlated with SPI while other indices exhibited both negative and positive correlations. Fig. 3a–e show the geographic distribution of significant asynchronous relationship between AMO, NINO 1.2, NINO 3, NINO 3.4, and NINO 4 indices and SPI (from 1 to 48 months) across the country, respectively. The number of significant relationships through asynchronous analysis was more than that of simultaneous analysis. Moreover, the highest correlation coefficients were observed for AMO, NINO 3.4, and NINO 4
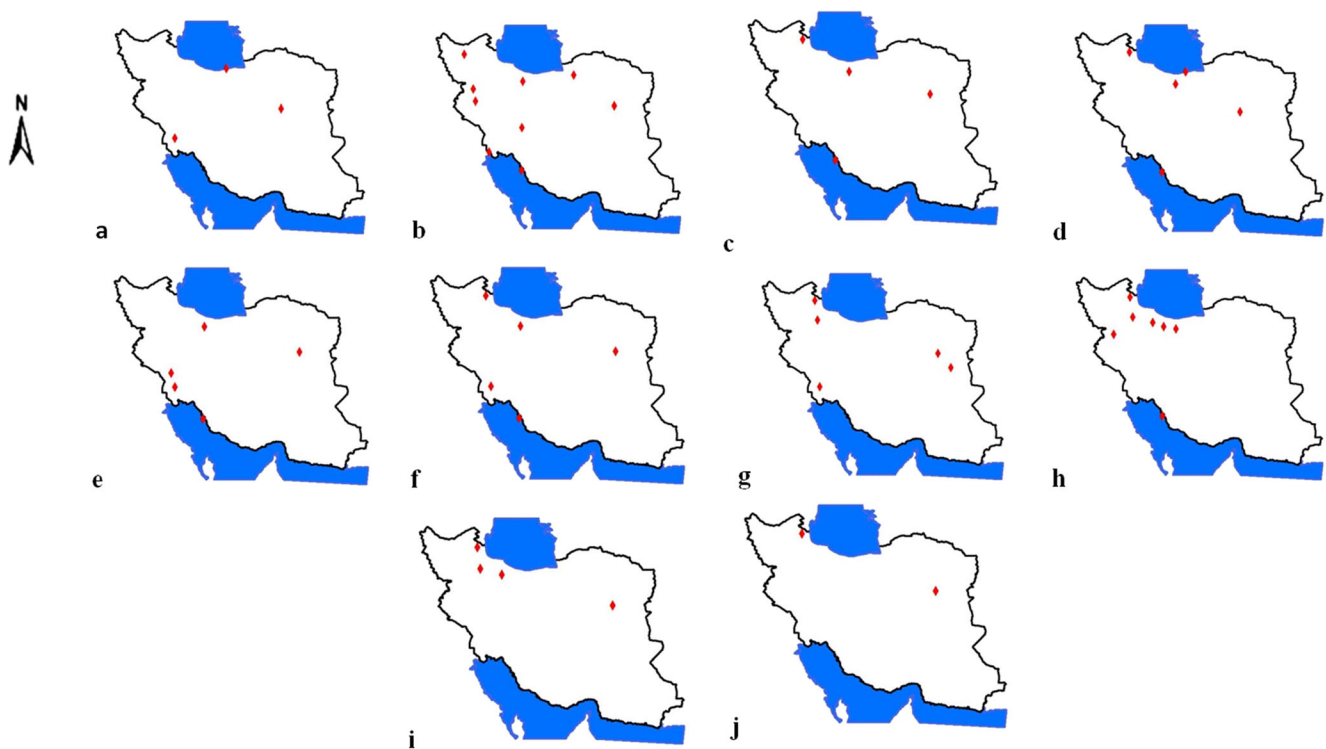

Fig. 2 Spatial pattern of Stations with simultaneous relationship to ocean-atmospheric indices in Iran: **a** AAO, **b** AMO, **c** AO, **d** NAO, **e** NINO 1.2, **f** NINO 3. **g** NINO 3.4, **h** NINO 4, **i** SOI, and **j** WeMo
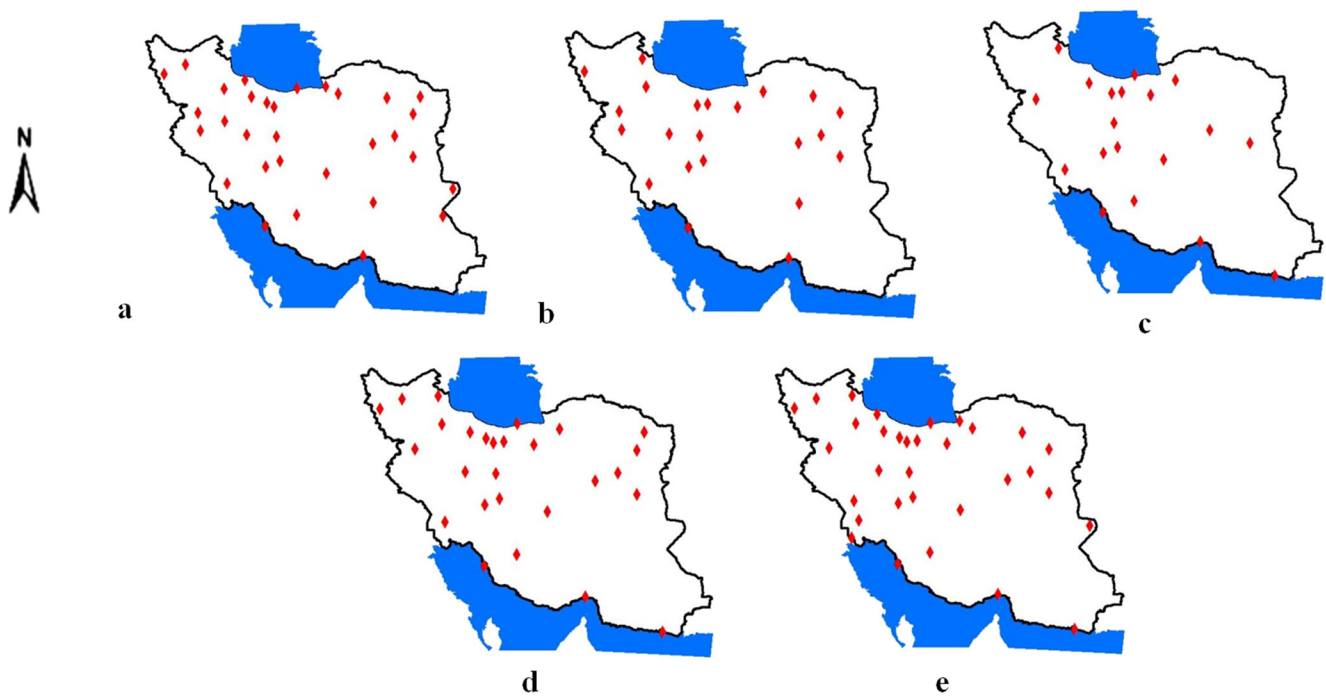
Fig. 3 Spatial pattern of stations with asynchronous relationship to ocean-atmospheric indices in Iran: **a** AMO, **b** NINO 1.2, **c** NINO 3, **d** NINO 3.4, and **e** NINO 4
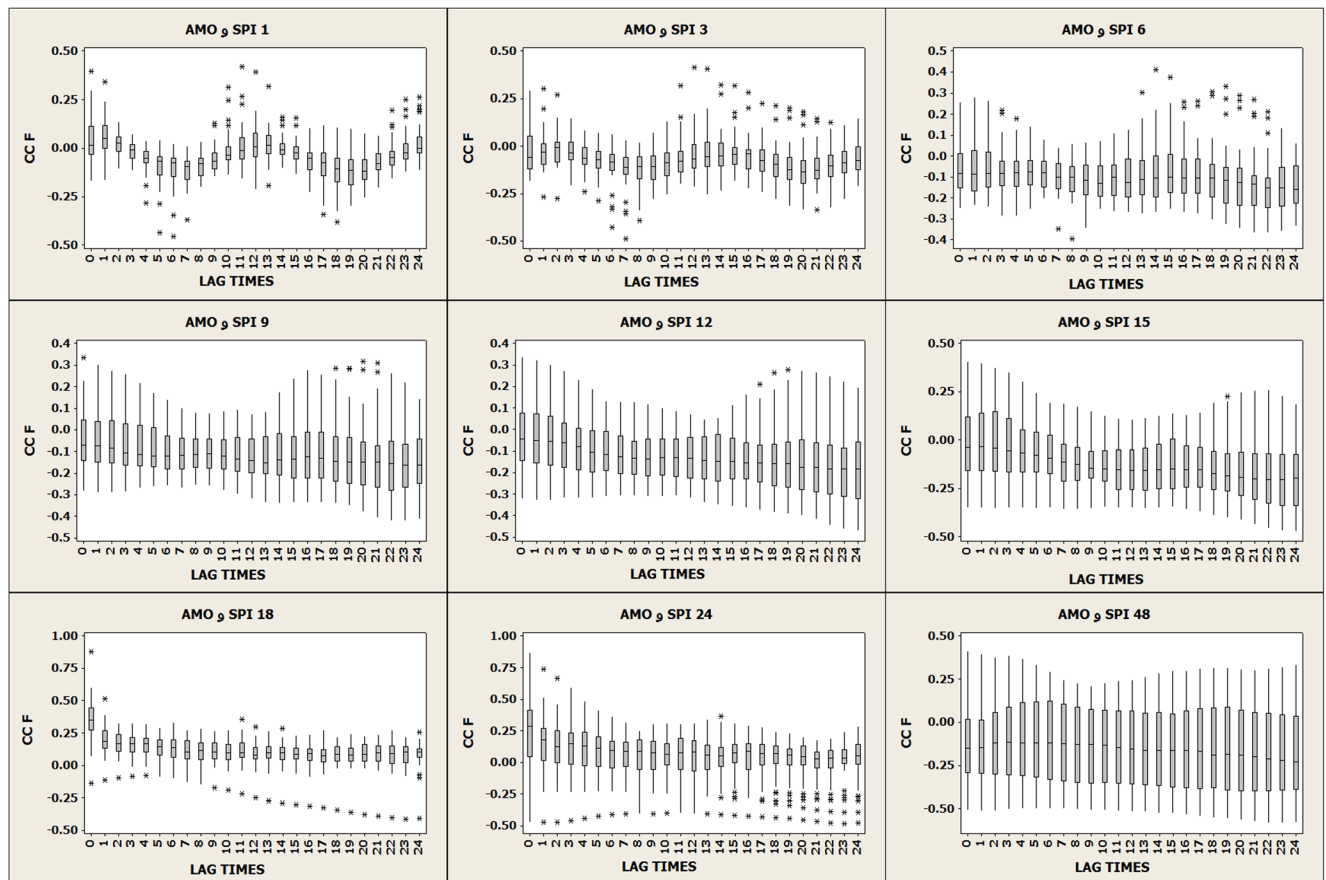

Fig. 4 Box plot of SPI values in different time scales stations with AMO index in lag time from 0 to 24 months ($\alpha = 0.05$)

indices across all stations except for southeastern ones. In general, significant relationships were more in the center, north, and west.

3.3 Boxplot

The boxplots of the cross-correlation coefficients between indices and SPI time series are given in Figures. 4, 5, and 6. In these figures, the horizontal axis is the lag time in months, and the vertical axis is the correlation coefficients between each SPI time series and the ocean-atmospheric indices. Figs. 4, 5, and 6 represent the boxplots of AMO, NINO 3.4, and NINO 4 at different SPI time scales respectively. Generally, the following assumptions should be taken into consideration when analyzing these relationships using boxplots which are:

(a) Outlier data represent the stations with extraordinary higher or lower correlation coefficients.
(b) The width of the box indicates the number of stations with a significant relationship. The number of stations with a significant relationship tends to increase due to increasing SPI time scales, indicating that ocean-atmospheric indices, especially AMO, NINO 3.4, and

NINO 4, have significant simultaneous and/or lagged impacts on precipitation and thus drought in Iran.
(c) Ocean-atmospheric indices are more significantly correlated with hydrological (SPI 9, 12) drought than the meteorological drought.

The NINO 3.4 and NINO 4 boxplots are similar to each other and differ from the AMO. In the AMO boxplots, most stations showed a significant time lag relationship. Moreover, the 48-month SPI produced no outlier and showed the highest correlation coefficients, indicating that with increasing lag of SPI, the time lag relationships become more significant and correlation coefficients do not change significantly over the lags. The AMO correlation coefficients appeared more concentrated around the mean value but differed between stations. In the NINO 3.4 and NINO 4 boxplots, correlation coefficients remained steady with increasing lag of SPI. In other words, periodic variation has occurred across all lag times and therefore, their correlation coefficients did not change significantly between lags and concentrated more around the mean value. Moreover, between 1- and 15-month SPI time scales in shorter lag times, the number of stations with a significant relationship was bigger than that in the higher lag times. In the 24-month SPI, the correlation
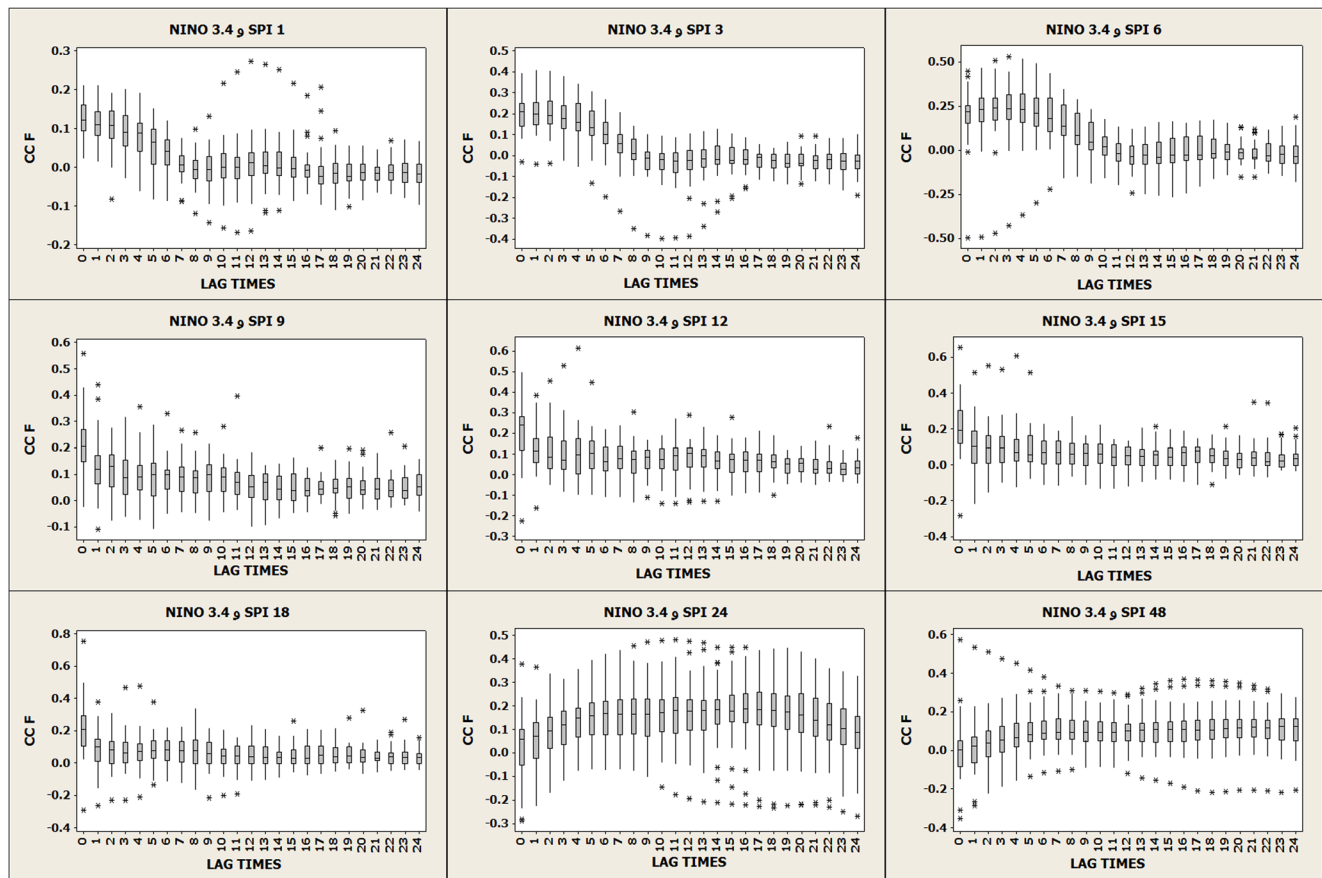

Fig. 5 Box plot of SPI values in different time scales stations with Nino 3.4 index in lag time from 0 to 24 months ($\propto = 0.05$)
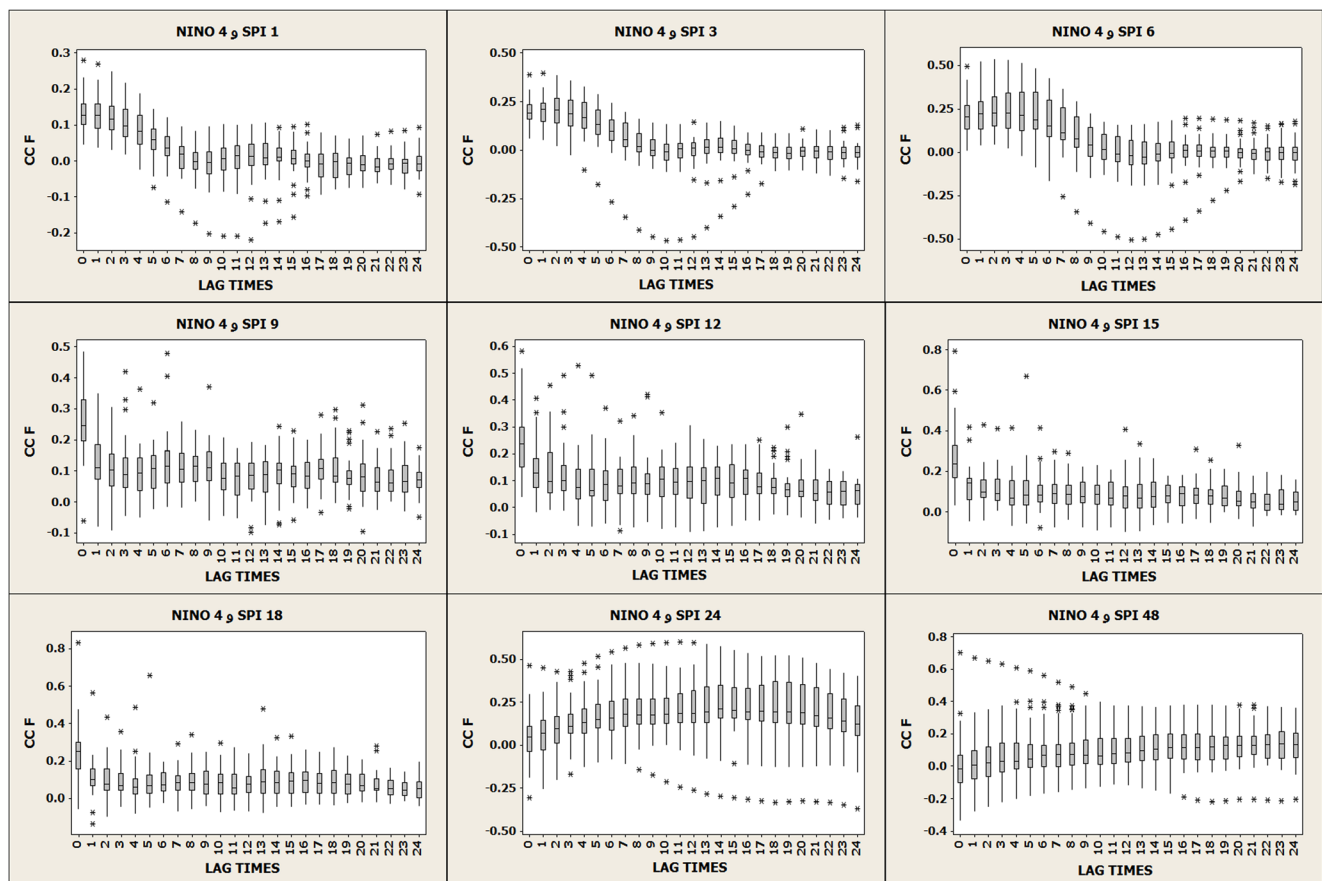
Fig. 6 Box plot of SPI values in different time scales stations with Nino 4 index in lag time from 0 to 24 months ($\propto = 0.05$)

coefficients and the number of stations with a significant correlation coefficient increased with increasing SPI lag.

In addition to the above results, positive outliers were identified in 3-, 6-, 12-, 24-, and 48-month SPI time scales. The relationship between the variables at the stations exhibiting outliers was either lower or higher than other stations. The frequency of the outliers was more in the stations located in the north and southwest of Iran including correlation of the AAO index with 3- and 6-month SPI at Babolsar, Bushehr, Dezful, and Gorgan stations (in the north and southwest), with 12-month SPI at Gorgan station (in the north), with 24-month SPI at Bushehr, Rasht, and Gorgan stations (in the southwest and north), and with 48-month SPI at Sabzevar station (in the northeast); moreover, the correlation of AMO index with 3-month SPI at Bushehr, Rasht, and Sabzevaar stations (in the north and southwest), with 6- and 12-month SPI at Gorgan and Rasht stations (in the north), with 24-month SPI at Bushehr Station (in the southwest); the correlation of AO index with 3-month SPI at Ardebil, Babolsar, Bushehr, Rasht, Sanandaj, and Gorgan stations (in the north and west), with 6-month SPI at Ardebil and Rasht stations (in the north), with 12-month SPI at Rasht station (in the north), and with 24-month SPI at Bushehr station (in the southwest); the correlation of NAO index with 3- and 6-months SPI at Rasht and Bushehr stations (in the northern and southwest), with 12-month SPI at Rasht station (in the north), and with 24-month SPI at Bushehr station (in the southwest); the correlation of NINO 1.2 index with 3-month SPI at Bushehr and Ferdows stations (in the southwest and northeast), with 6-month SPI at Bushehr, Sabzevar, Ferdows, and Gorgan stations (in the southwest and north), with 12- and 48-month SPI at Bushehr station (in the southwest), and with 24-month SPI at Ferdows station (in the northeast); the correlation of NINO 3 index with 3- and 6-month SPI at Sabzevar station (in the northeast), with 12-month SPI at Arak, Bushehr, and Gorgan stations (in the center, west, and north), with 24-month SPI at Ardebil station (in the northwest), and with 48-month SPI at Rasht and Gorgan stations (in the northern); the correlation of NINO 3.4 index with 6-month SPI at Ferdows station (in the northeast), with 12- and 48-month SPI at Bushehr station (in the southwest), and with 24-month SPI Shahrekord station (in the west); the correlation of NINO 4 index with 3-month SPI at Sanandaj station (in the west), with 6-month SPI at Shahrekord station (in the western), with 12- and 24-month SPI at Abadan and Bushehr stations (in the southwest), with 24-month SPI at Arak station (in the center), and with 48-month SPI at Bushehr station (in the southwest); the correlation of SOI index with 3-month SPI at Gorgan station (in the

north), with 6-month SPI at Babolsar station (in the north), with 12-month SPI at Bushehr station (in the southwest), and with 24- and 48-month SPI at Karaj and Gorgan stations (in the north); and the correlation of WeMo index with 3-month SPI at Abadan and Bushehr stations (in the southwest), with 6- and 12-month SPI at Gorgan station (in the north), and with 24-smonth SPI at Yazd station (in the center).

3.4 Regression analysis

Ocean-atmospheric indices were considered as the independent variables, and different SPI time scales were considered as the dependent variables. The ocean-atmospheric indices were entered into the equations using simultaneous and 1-, 2-, 3-, 4-, 5-, 6-, 12-, 24-, and 48-month lag. Nine regression equations were developed for each station (according to the 9 SPI time scales) which contained ten ocean-atmospheric indices.

In the SPI equations, the predictor variables, which were oceanic-atmospheric indices at one simultaneous and different time lag modes, were entered to equations based on the location of stations and time scales. For example, the SPI6 equation at Mashhad Station is presented in Eq. 3 in which eight variables were chosen including Nino 3.4 with a 5-month lag, Nino 4 with a 48-month lag, Amo with a 0-month lag, SOI with a 5-month lag, AMO with a 12-month lag, SOI with a 6-month lag, Nino 1.2 a 24-month lag, and Nino 1.2 a 48-month lag.

$$\text{SPI6 (Mashhad station)} = 0.312\text{lag5 NINO3.4} \quad (3)$$

$$-0.244\text{lag48 nino4} - 1.003\text{lag0 AMO} - 0.094\text{lag5 SOI}$$

$$+ 0.479\text{lag12 AMO} - 0.083\text{lag6 SOI} - 0.101\text{lag24 NINO1.2}$$

$$-0.084\text{lag48 NINO1.2} + 0.007$$

Table 2 The number of used variables in the simultaneous and asynchronous relationships of regression equations

The number of simultaneous indices entered into the regression model	The number of lag timed indices entered into the regression model	Standardized Precipitation Index in time scales
32	205	1
24	301	3
63	373	6
61	394	9
57	414	12
75	463	15
85	418	18
77	463	24
74	493	48

In order to select the best regression model, the regression coefficient (R), R^2, RMSE, and CE were calculated at each station for each SPI time scale. The highest R, R^2, and CE and the lowest RMSE values were observed at the Bushehr station for 1-, 3-, 12-, 15-, 18-, 24-, and 48-month SPI.

Table 2 shows the number of variables entered into each regression equation through simultaneous and time lag modes. These results showed that as the SPI time scale increases, a relatively larger number of variables through both simultaneous and lag time modes were entered into the equations and resulted relationships became more significant. After extracting the regression equations, the validity of the models was tested by comparing the observed and predicted values obtained at each station and different SPI time scales. The results are presented in Table 3. According to CE and R values (0.6–1), the models were well fitted and showed no overfitting.

4 Discussion and conclusion

This study assessed the teleconnection effect of ocean-atmospheric indices on precipitation and consequently on drought in Iran. The results achieved in this study are as follows:

– In the simultaneous mode, 18 stations showed a significant relationship between SPI and ocean-atmospheric indices. In terms of frequency, NINO 1.2, NINO 3, and NINO 4 and then AMO, AO, and NINOs showed the highest relationships with different SPI time scales while in terms of the number of stations, AMO and NINO 4 outperformed other indices.

Regarding the geographic distribution of the stations, the highest correlation coefficients were between SPI and NAO, NINOs (NINO 1.2, NINO 3, NINO 3.4, and NINO 4), AAO, and AMO in the north and between SPI and AO, NAO, SOI, AMO, and NINOs (except NINO 1.2) in the northwest. Moreover, except for the relationship of SPI with SOI and WeMo in the southwest and AMO in the center, all indices were correlated.

According to our results, Salahi et al. (2005) showed that the precipitation had a weak negative relationship with NAO in northwestern Iranian stations (Tabriz, Ahar, and Jolfa stations) especially during widespread drought and wet years.

– In the lag time mode, significant positive or negative relationships were found between SPI and ocean-atmospheric indices in 35 (out of 37) stations. Five indices (out of 10) showed a significant time lag relationship

Table 3 Statistics of error for SPI6-SPI48 in study region

Type of error Station	SPI6		SPI9		SPI12		SPI15		SPI18		SPI24		SPI48	
	CE	R	CE	R	CE	R	CE	R	CE	R	CE	R	CE	R
Abadan	0.5740	0.7576	0.6240	0.7900	0.7012	0.8374	0.6654	0.8157	0.7145	0.8453	0.7966	0.8925	0.7043	0.8392
Abali	0.4374	0.6614	0.4042	0.6358	0.4649	0.6819	0.4787	0.6919	0.4470	0.6686	0.4256	0.6523	0.5126	0.7160
Ahvaz	0.3427	0.5854	0.4501	0.6709	0.5269	0.7259	0.5870	0.7662	0.6229	0.7893	0.5792	0.7611	0.6678	0.8172
Arak	0.3572	0.5992	0.3590	0.5992	0.5759	0.7589	0.6579	0.8111	0.4587	0.6799	0.5553	0.7452	0.6283	0.7927
Ardebil	0.3761	0.6133	0.4642	0.6813	0.4990	0.7064	0.5554	0.7453	0.5019	0.7084	0.4907	0.7005	0.5890	0.7675
Babolsar	0.5393	0.7344	0.6115	0.7820	0.6434	0.8021	0.6580	0.8112	0.6368	0.7980	0.6448	0.8030	0.8208	0.9060
Bandar abas	0.2104	0.4586	0.2392	0.4891	0.3128	0.5593	0.3597	0.5998	0.4189	0.6472	0.4868	0.6977	0.5994	0.7742
Birjand	0.4042	0.6358	0.4015	0.6336	0.4296	0.6554	0.4662	0.6828	0.4784	0.6916	0.5337	0.7306	0.7254	0.8517
Boshehr	0.0094	0.5826	0.0202	0.5896	0.8998	0.9486	0.9062	0.9520	0.9351	0.9670	0.9975	0.9988	0.8709	0.9332
Chabahar	0.0101	0.1248	0.2351	0.2847	0.5695	0.5999	0.4574	0.3254	0.6974	0.7415	0.5901	0.6475	0.6451	0.7451
Dezfol	0.4989	0.7064	0.6510	0.8068	0.7178	0.8472	0.7981	0.8934	0.7854	0.8862	0.8080	0.8989	0.6497	0.8061
Esfahan	0.5167	0.7188	0.5092	0.7135	0.6548	0.8092	0.6154	0.7845	0.6983	0.8357	0.7173	0.8470	0.6377	0.7986
Ferdos	0.3599	0.5999	0.5413	0.7357	0.5668	0.7529	0.6652	0.8156	0.5748	0.7581	0.6325	0.7953	0.8103	0.9001
Ghazvin	0.4542	0.6739	0.4812	0.6937	0.4810	0.6936	0.5496	0.7414	0.4426	0.6653	0.4856	0.6969	0.5107	0.7146
Gorgan	4.6166	0.0647	0.9753	0.9876	0.9507	0.9750	2.5521	0.3489	3.2529	0.2984	0.9853	0.9926	4.8434	0.0294
Hamedan	0.3951	0.6286	0.5448	0.7381	0.4875	0.6982	0.5580	0.7470	0.5141	0.7170	0.5348	0.7313	0.5642	0.7512
Karaj	0.4036	0.6353	0.3880	0.6229	0.4729	0.6877	0.6561	0.8100	0.5637	0.7508	0.5112	0.7150	0.5561	0.7457
Kashan	0.2998	0.5475	0.3359	0.5795	0.4191	0.6474	0.4093	0.6397	0.3132	0.5596	0.3849	0.6204	0.3440	0.5865
Kerman	0.1770	0.4207	0.2654	0.5153	0.3363	0.5799	0.3616	0.6013	0.3835	0.6200	0.4835	0.6954	0.6082	0.7799
Kermanshah	0.4533	0.6733	0.4924	0.7017	0.5180	0.7197	0.5675	0.7533	0.6291	0.7931	0.6374	0.7983	0.7091	0.8421
Mashhad	0.3601	0.6001	0.3997	0.6322	0.4601	0.6783	0.4812	0.6937	0.5275	0.7263	0.6237	0.7897	0.7671	0.8759
Urmia	0.3495	0.5981	0.4539	0.6737	0.4907	0.7005	0.4955	0.7039	0.5327	0.7299	0.5519	0.7429	0.5399	0.7348
Rasht	0.5566	0.7460	0.5879	0.7667	0.6546	0.8091	0.6410	0.8006	0.4862	0.6973	0.6415	0.8009	0.8841	0.9403
Sabzevar	0.4939	0.7028	0.7460	0.6899	0.5096	0.7139	0.5293	0.7275	0.4857	0.6969	0.4502	0.6710	0.4997	0.7069
Sanandaj	0.6394	0.7996	0.6106	0.7814	0.5717	0.7561	0.6668	0.8166	0.6751	0.8217	0.6907	0.8311	0.6484	0.8052
Semnan	0.3771	0.6141	0.3454	0.5877	0.3922	0.6262	0.4081	0.6388	0.3640	0.6033	0.4045	0.6360	0.2513	0.5013
Shahhrod	0.3263	0.5712	0.3820	0.6181	0.3790	0.6158	0.4523	0.6726	0.4935	0.7025	0.4996	0.7068	0.6031	0.7766
Shahrekord	0.5931	0.7701	0.7000	0.8385	0.7658	0.8751	0.7253	0.8517	0.7387	0.8595	0.7438	0.8624	0.7438	0.8624
Shiraz	0.3022	0.5497	0.3479	0.5899	0.4178	0.6464	0.4973	0.7052	0.5164	0.7186	0.6328	0.7955	0.7542	0.8685
Tabas	0.3178	0.5638	0.4914	0.7010	0.5246	0.7243	0.5742	0.7577	0.5633	0.7505	0.5478	0.7401	0.7210	0.8491
Tabriz	0.4206	0.6203	0.5336	0.7305	0.5374	0.7331	0.5229	0.7231	0.5147	0.7175	0.4875	0.6982	0.4964	0.7046
Tehran	0.4371	0.6611	0.3356	0.5793	0.4381	0.6691	0.4372	0.6612	0.4022	0.6342	0.4074	0.6383	0.4665	0.6830
Torbat	0.2347	0.4845	0.2970	0.5449	0.3316	0.5759	0.3958	0.6291	0.3962	0.6294	0.4450	0.6671	0.5644	0.7513
Yazd	0.3044	0.5519	0.4120	0.6419	0.4507	0.6713	0.4806	0.6933	0.4925	0.7018	0.5893	0.7677	0.7188	0.8478
Zabol	0.3193	0.5651	0.3696	0.6080	0.3944	0.6281	0.4557	0.6751	0.4397	0.6631	0.5928	0.7699	0.6360	0.7975
Zahedan	0.1635	0.4043	0.2357	0.4854	0.2744	0.5238	0.3599	0.5999	0.4531	0.6731	0.5293	0.7275	0.5217	0.7223
Zanjan	0.3642	0.6035	0.3247	0.5698	0.3306	0.5750	0.3770	0.6140	0.3428	0.5855	0.2523	0.5034	0.2841	0.5330

between SPI and AO, AAO, NAO, SOI, but the WeMo did not show a significant relationship.

NINO 3.4 and NINO 4 had positive relationships and AMO, NINO 3, and NINO 1.2 had both positive and negative relationships. AMO, NINO 4, and NINO 3.4 indices were the most widely used indices at the stations and had significant lag time relationships with SPI.

With increasing SPI time scales, ocean-atmospheric indices with longer lag times are more effective in drought. This highlights that, firstly, these indices affect drought in Iran with time lag patterns and, secondly, there is a direct relationship between SPI time scales and lag times in these indices. In both simultaneous and time lag modes, drought in the eastern and southeastern regions of Iran was not affected by any OA oscillation indices. The results of this study are consistent

with the previous research findings. For instance, Roughani et al. (2010) studied the seasonal scale relationship between ocean-atmospheric indices and precipitation in Iran and concluded that there is a negative relationship between autumn precipitation and SOI for 0- to 2-month time lags, especially in northwestern parts of Iran.

Our study showed that significant relations of ENSO indices including NINO 1.2, NINO 3, NINO 3.4, and NINO 4 with drought had a proper distribution in Iran while the relationship between SOI and droughts was not significant at any station. Also, it was found that NAO in December, with a 6-month lag, had a negative and significant correlation with January drought at northern Iranian stations in the south of the Caspian Sea (Bandar Anzali, Rasht, Ramsar, and Noshar). Furthermore, January NAO, with a 4-month lag, had a negative significant relationship with May precipitation in southwestern stations (Dezful and Ahvaz). WeMo also had significantly negative simultaneous and 1-month relationships with winter precipitation. Winter precipitation was significantly correlated with SPI at all stations except eastern and southeastern Iranian stations. WeMo and NAO showed no significant relationships with SPI in any station.

– The highest regression coefficients were observed for 0-, 1–6-, 12-, 24-, and 48-month lags. AMO, NINO 4, NINO 3.4, and NINO 3 had the largest number of significant relationships. Moreover, with increasing SPI time scale, ocean-atmospheric indices with longer lags were entered into the regression equations. At different SPI time scales, various lag times imposed different impacts. At 1- and 3-month SPIs, 0-, 1-, 5-, and 6-month lags were more effective, and the highest frequency was observed in a 6-month time lag. At 6- to 12-month SPIs, the largest number of significant lags was observed for 12- and 24-month lags. At 18- to 48-month SPIs, the largest number of significant lags was observed for 12- and 24-month lag times. The results of model validation showed no overfitting in the regression models. In agreement with our results, Yarahmadi and Azizi (2008) found that, among the ENSO-based indices, NINO 3.4 had the highest positive relationship with autumn and winter precipitation in Iran. According to these findings, the significant relationship between ocean-atmospheric indices and SPI showed that drought is more associated with time lag effects of ocean-atmospheric oscillations.

Overall, the study indices had significant lag time impacts on precipitation and drought at western and northwestern stations which can be attributed to the effect of air masses coming from the Mediterranean Sea to Iran. Iran does not have considerable in-land water bodies. Hence, the amount of water vapor needed for precipitation enters Iran from nearby water sources, such as the Caspian Sea and southern open waters and also distant water resources such as Mediterranean Sea, Black Sea, Red Sea, and Bengal Bay, and general global–regional atmospheric circulation systems, and is distributed according to local factors. This indicates that the spatio-temporal distribution of moisture is affected by both local and regional factors.

The significant AMO-SPI relationship can be due to the proximity of the Mediterranean Sea to the Atlantic Ocean and the Atlantic high-pressure systems that bring precipitation to Iran by western winds over the Mediterranean Sea.

In cold seasons, all pressure systems including high-level waves and in-land circulations enter Iran due to the established Mediterranean low pressure (Alijani 1995). In this case, our findings are consistent with those of Nazemosadat and Mostafa Zadeh (2014) who found that the frequency of dry and wet periods in most parts of Iran was related to the positive and negative phases of AMO, respectively.

Also, due to the impact of ENSO-based indices including NINO 1.2, NINO 3, NINO 3.4, and NINO 4 on drought, it can be concluded that drought occurrence in Iran is more related to the global effect of ENSO and its complex interaction with other large-scale ocean-atmospheric indices.

The results of this study corroborate those of Qaed Amini et al. (2014) who found that ENSO governs precipitation oscillations in southwestern Iran. This finding necessitates further studies to elucidate the behavior effect of ENSO, as one of the most important teleconnection drivers, on various climatic aspects of Iran. The relationship of this index with other teleconnection indices can be of great help for long-term prospects. The global influences of ENSO have more impacts on precipitation and drought patterns in northern Iranian stations. In the west and southwest of Iran, contrarily, precipitation and drought patterns are more influenced by Khamsin's low-pressure masses and Sudanese flows.

Despite the proximity of southern and southeastern parts of the country, such as Bandar Abbas, Chabahar, Zahedan, and Zabol stations to the open waters of the Persian Gulf and the Oman Sea, the relationship between indices and SPI was not statistically significant. One possible explanation for this could be the impacts of the water surface temperature of the Persian Gulf, Oman Sea, Indian Ocean, and Indian monsoon currents on these areas.

5 Recommendations for future studies

Considering that AMO showed the highest impact on drought in both simultaneous and asynchronous modes at Bushehr and southern stations, using the data of nearby Persian Gulf stations including Dubai and the United Arab Emirates to continue the study in this case is suggested.

In addition, considering the significant relationship between SST and rainfall based on sea surface temperature of the Persian Gulf, studying the relationship between SSTs at

the water borders of Iran about droughts is recommended. Also, other atmospheric ocean indices are to be used for better research in various parts of Iran's stations.

References

Alijani, B. (1995). The climate of Iran, Tehran, publisher of Payam Noor University

Azhdari Moghaddam M, Khosravi M, Pour Niknam H, Jafari Nadoushan A (2012) Prediction of Drought using fuzzy-neural model, climatic indices, rainfall and drought index (case study: Zahedan). Quarterly Journal of Geography and Development 26:61–72

Darand M (2014) Drought monitoring of Iran by Palmer Drought Index and its relation to atmospheric-oceanic teleconnection patterns. Quarterly Journal of Geographic Research 4(13):82–67

Dezfuli AK, Karamouz M, Araghinejad S (2010) On the relationship of regional meteorological drought with SOI and NAO over southwest Iran. Theor Appl Climatol 100(1):57–66

Dinpashoh Y, Fakheri-Fard A, Moghadamnia M, Jahanbakhsh S, Mirnia M (2004) Selection of variables for the purpose of regionalization of Iran's precipitation climate using multivariate methods. J Hydrol 297:109–123

Ghasemi AR, Khalili D (2008) The association between regional and global atmospheric pattern and winter precipitation in Iran. Atmos Res 88:116–133

Halabian, A. (2016). Estimation of rainfall spatial and temporal variations in Iran, desert ecosystem engineering journal, Year 5, No13, pp. 101–116

Jafarzadeh, F., Salahi, B., Sobhani, B. (2009). Evaluating effect of ENSO on the droughts and wetness of Ardabil Province, Master's Thesis, Department of Literature and Humanities, University of Mohaghegh Ardabili

Khosravi M (2004) Evaluating relationship between north-hemisphere large-scale atmospheric circulation patterns with annual droughts in Sistan and Baluchestan. Geography and development magazine 2(3):167–188

Komuscu AU (2001) An analysis of recent drought conditions in Turkey in relation to circulation patterns. Drought Network News 13(2–3): 5–6

Lim YK, Kim KY (2007) ENSO impact on the space-time evolution of the regional Asian summer monsoons. J Clim 20:2397–2415

Lyon B (2005) ENSO and the spatial extent of interannual precipitation extremes in tropical land areas. Journal of climate 18:5095–5109

Masoudian, SA. (2011). Iran's climate, Mashhad toos publishing, Mashhad, first edition, autumn 2011, Mashhad

Matyasovszky I (2003) The relationship between NAO and rainfall in Hungary and its nonlinear connection with ENSO Theor. Appl.Climatol. 76:69–75

McCabe, GJ. Betancourt, JL., Gray, ST., Palecki, MA. Hidalgo, HG. (2008. (Associations of multi-decadal sea-surface temperature variability with US drought. Quaternary International, 188:31–40

McKee, TB. Doesken, NJ. Kleist, J. (1993)."The relationship of drought frequency and duration to time scales", 8th conference on Applied Climatology, 17–22 January, Anaheim, pp. 176–184

Modarres R (2006) Regional precipitation climates of Iran. J Hydrol 45: 13–27

Mokhtari, A., Islamian, SS., Mousavi, SF. (2012). Evaluation of drought indices and oscillations in Iran with indicators of oceanic oscillations, master's degree of irrigation and drainage, Department of Agriculture, Isfahan University of Technology

Nazemosadat, MJ., Ghasemi, A. (2002). Drought and excess rainfall in Sistan and Baluchestan and its relation with the El Niño - south oscillation. Collection of the articles' first conference on reviewing the water crisis response strategies, pp 24–31

Nazemosadat, MJ., Mostafa Zadeh, K.. (2014). Effect AMO phenomenon on the fluctuation of winter rainfall and the occurrence of dry and wet periods of Iran, second National Conference of water Crisis, Shahrekord of University

Negaresh H, Armesh M (2011) Using the neural network for drought forecasting in Khash. Geographic Studies of Arid Regions 6:33–50 (in Farsi)

Nikzad M, Behbahani khub, A. (2013) Detection of dependencies between ocean-atmospheric and climatic parameters for drought monitoring using data (case study: Khuzestan province). Journal of Iran Water Research 7(13):175–183

Oladipio EO (1985) A comparative performance analysis of three meteorological drought indices. Int J Climatol 5:655–664

Partridge, IJ. (2001. (Will it rain? The effects of the southern oscillation and El Nino on Australia,3ed :Dept. of primary industries, Brisbane

Qaed Amini H, Nazemosadat MJ, Kuhizadeh M, Sabziparvar A (2014) Separate and simultaneous demonstration of PDO and ENSO phenomena on drought and wetness occurrence in southern Iran. Iranian Geophysics Journal vol. 8(2):92–109

Razei, T., Daneshkar-Arasteh P., Saghfian, B. (2005). "Annual rainfall trend in arid (Oder) and semi-arid regions of Iran", *in ICID 21st European Regional Conference*, Frankfurt, Germany, and Słubice, Poland, pp 20–28

Roughani, R., Soltani, S., Bashari, h. (2010). Investigation of rainfall changes in Iran with oceanic-atmospheric indices, master's thesis of watershed management, Department of Natural Resources, Isfahan University of Technology

Salahi B, Hajizadeh Z (2013) Analysis on temporal relation of North Atlantic oscillation and Atlantic surface temperature indexes with variability of precipitation and temperature in Lorestan Province. Quarterly journal of geographic research 3:117–128

Salahi B, Khorshiddost A, Ghavidel Rahimi Y (2005) Relationship northern Atlantic oceanic circulation oscillation with East Azarbaijan droughts. University of Tehran, Geographical Research 60:156–147

Salas JD (1993) Analysis and modeling of hydrologic time series. In: Maidment DR (ed) Handbook of hydrology. McGraw Hill, New York, pp 19.1–19.72

Shimizu M, Ambrizzi T (2015) MJO influence on ENSO effects in precipitation and temperature over South America. Theor Appl Climatol 124(1):291–301

Thom HCS (1958) A note on the gamma distribution. Mon Weather Rev 86:117–122

WWW. http://co-public.lboro.ac.uk/cocwd/HydroTest/Details.html. Accessed June 2017

WWW.bom.gov.au/climate. Accessed January 2017

WWW.cpc.ncep.noaa.gov. Accessed January 2017

WWW.esrl.noaa.gov/psd/data/climateindices/list Accessed January 2017

WWW.irimo.ir. Accessed December 2016

Yarahmadi D, Azizi Q (2008) Analysis multivariable of seasonal precipitation of Iran and climate indices. Geogr Res 39(62):161–174